Articles in PresS. J Neurophysiol (November 30, 2005). doi:10.1152/jn.01050.2005

Title: **The awake behaving worm: simultaneous imaging of neuronal activity and behavior in intact animals at millimeter scale**

Authors: **Serge Faumont and Shawn R. Lockery**

Affiliation: **Institute of Neuroscience, University of Oregon, Eugene, OR 97403, USA**

Running head: **The awake behaving worm**

Contact information: Shawn Lockery, 1254 University of Oregon, Eugene, OR 97403, shawn@lox.uoregon.edu, phone: 541-346-4590, fax: 541-346-4548

Abstract

Genetically encoded optical probes of neuronal activity offer the prospect of simultaneous recordings of neuronal activity and behavior in intact animals. A central problem in simultaneous imaging is that the field of view of the high power objective required for imaging the neuron is often too small to allow the experimenter to assess the overall behavioral state of the animal. Here we present a method that solves this problem using a microscope with two objectives focused on the preparation: a high power lens dedicated to imaging the neuron and low power lens dedicated to imaging the behavior. Images of activity and behavior are acquired simultaneously but separately using different wavelengths of light. The new approach was tested using the cameleon calcium sensor expressed in *C. elegans* sensory neurons. We show that simultaneous recordings of neuronal activity and behavior are practical in *C. elegans* and, moreover, that such recordings can reveal subtle, transient correlations between calcium levels and behavior that may be missed in non-simultaneous recordings. The new method is likely to be useful whenever it would be desirable to record simultaneously at two different spatial resolutions from a single location, or from two different locations in space.

Key words

C. elegans, cameleon, chemosensation, genetically encoded optical probe

Introduction

Genetically encoded optical probes of neuronal activity offer the prospect of simultaneous recordings of neuronal activity and behavior in intact animals. These include optically transparent, genetically tractable organisms such as nematodes (Kerr et al. 2000) and larval zebra fish (Higashijima et al. 2003), and also opaque organisms such as the fruit fly and mouse, in which the brain can be exposed by localized dissection (Fiala et al. 2002; Hasan et al. 2004; Ng et al. 2002). A wide range of probes have been developed that monitor key markers of neuronal activity such as transmembrane voltage, intracellular calcium, and synaptic vesicle cycling (Guerrero and Isacoff 2001; Miesenbock 2004; Miesenbock and Kevrekidis 2005; Miyawaki 2003). Nevertheless, the potential for using optical probes to record neuronal activity and behavior simultaneously remains largely untapped.

A central problem in imaging neuronal activity and behavior simultaneously is that the field of view of the high power objective required for imaging the neuron is often too small to allow the experimenter to see more than a small portion of the animal. Thus it is generally not possible to ascertain, with confidence, the behavioral state of the animal throughout an imaging session. Here we present a method that solves this problem using a microscope with two objectives focused on the preparation: a high power lens dedicated to imaging the neuron and a low power lens dedicated to imaging the behavior. Images of activity and behavior are acquired simultaneously but separately using different wavelengths of light.

The new approach was developed in connection with the probe known as cameleon, a calcium sensitive relative of green fluorescent protein (Miyawaki et al. 1999; Miyawaki et al. 1997). Cameleon is a chimeric protein comprised of two derivatives of green fluorescent protein—cyan fluorescent protein (CFP) and yellow fluorescent protein (YFP)—bridged by calmodulin and the calmodulin binding domain of myosin light chain kinase (M13). In the presence of calcium, calmodulin binds to M13, which brings CFP and YFP closer to each other. When the molecule is excited at wavelengths that activate CFP, close apposition of CFP and YFP increases the efficiency of fluorescence resonance energy transfer between them, leading to an increase in the ratio of yellow to cyan fluorescence. A key strength of the cameleon protein is that it can be targeted to the neuron of interest by a cell-specific promoter for positive identification of the cell.

We used the new method to study the relationship between neuronal activity and behavior in *C. elegans*. In the past, the small size of the animal (1 mm in length) and its neurons (2 μm in diameter)—together with its tough, pressurized cuticle—was a barrier to neurophysiological analysis. This situation changed with the advent of four new techniques: (1) sharp-electrode recordings from pharyngeal muscle (Davis et al. 1995), (2) whole-cell patch clamp recordings from neurons and muscles in situ (Goodman et al. 1998; Richmond and Jorgensen 1999), (3) a method for culturing *C. elegans* neurons (Christensen et al. 2002) and (4) calcium imaging from neurons and muscles using genetically encoded probes (Kerr et al. 2000; Suzuki et al. 2003). However, it has not so far been possible to make simultaneous recordings of neuronal activity and whole-

animal behavior in *C. elegans*, a significant obstacle to a comprehensive neuroethology of this widely studied genomic organism.

We present evidence that simultaneous recordings of neuronal activity and behavior are practical and illuminating in *C. elegans*. We found that calcium signals can be detected reliably in animals that are only partially immobilized and that such animals continue to respond behaviorally to chemosensory stimulation despite the presence of cameleon. We also found that simultaneous recording can reveal subtle correlations between neuronal activity and behavior that may be difficult to detect in non-simultaneous recordings.

Materials and Methods

Optics. To make simultaneous recordings of neuronal activity and behavior, we used an inverted microscope (Zeiss Axiovert 135) with two objective lenses focused on the preparation: a high power objective below the microscope stage, and a low power objective above the microscope stage (Fig. 1). We refer to this as the dual-objective approach. The high power objective (63x oil, 1.4 NA), situated on the nosepiece of the microscope, was used for calcium imaging. The low power objective (10x, 0.25 NA, 160 mm tube length), supported by a hinged platform, formed an image of the whole animal for an analog video camera (Sony XC-ST70, Ft. Meyers, FL, USA) that was used to record behavior to video tape. The purpose of the hinged platform was to enable the experimenter to interchange the low power objective with the microscope's condenser for bright-field illumination when arranging the preparation on the microscope stage. A three-axis manipulator (not shown), incorporated into the hinged platform, was used to center and focus the low power objective. The microscope was equipped with an epifluorescence illuminator, software-controlled shutter (ASI, Eugene, OR), beam splitter (Optical Insights, OI-DV-FC, Tucson, AZ, USA) and digital video camera (Hamamatsu, ORCA-AG, Bridgewater, NJ, USA) for ratiometric calcium imaging using cameleon as previously described (Kerr et al. 2000; Suzuki et al. 2003).

The optics contained two other key components. The first component was a 575 nm long-pass filter inserted between the low power objective and the behavior camera. The function of this filter was to prevent saturation of the behavior camera by the intense

blue light (426-446 nm) used to excite the cameleon protein. The second component was a red laser (635 nm, 4.9 mW) that served to illuminate the animal. We selected a red laser to avoid interference with the emission wavelengths of the cameleon protein (465-555 nm). Contrast in the behavior image was enhanced by aiming the laser beam almost parallel to the microscope stage. This arrangement minimized specular reflection from the polished surface of the high power objective and achieved a pseudo dark-field illumination effect; we were unable to obtain sufficient contrast using light emitting diodes aimed at the preparation. The behavior of the animal, as assessed with bright-field illumination, did not visibly change when the laser was turned on or off. We synchronized the calcium imaging and behavior recordings manually. This synchronization was achieved by starting the video tape recording, then simultaneously activating the laser and the software routine that opened the shutter to begin frame acquisition for calcium imaging. We found that shutter opening was delayed relative to laser activation because of latencies in software. We measured this delay by removing the long-pass filter normally inserted between the low power objective and the behavior camera so that this camera was now saturated whenever the shutter opened. Video data from the behavior camera was then replayed frame by frame to measure the time between laser activation (the start of the behavior record) and shutter opening (the start of the calcium imaging record). We observed a delay of 0.75 ± 0.01 s (mean ± SEM, n = 14); all calcium imaging and behavior recordings were therefore aligned in time by deleting the first 0.75 sec from the behavior record. Additionally, the low variability in the delay indicated that experimenter reaction times were negligible.

Animals. We used adults of the strain AQ1444 (*lin-15(n765)* X; ljEx95 [*lin-15(+)*; p*sra-6*::YC2.12]), in which cameleon is expressed specifically in the ASH sensory neurons (Hilliard et al. 2005). The previously reported weak expression in the ASI sensory neurons (Troemel et al. 1995) was not observed; thus, we were able to identified ASH neurons unambiguously. The emission intensity of the cameleon protein varied between individual animals, a likely consequence of the fact that the cameleon construct exists as an extrachromasomal array in this strain. In this study, we focused on animals in which expression was judged by eye to be bright enough to give good calcium signals.

Preparation and solutions. To stabilize worms for recording, we used the so-called glued worm preparation (Faumont et al. 2005), in which animals are glued to agarose coated coverslips and submerged in a pool of saline. The glue is confined to the region of the head such that the head remains relatively still whereas rest of the body is free to move. The coverslip is sealed with wax under a hole in a glass plate, forming a recording chamber, which is filled with saline.

We have shown previously that worms prepared in this way exhibit recognizable components of locomotory behavior and respond normally to chemosensory inputs (Faumont et al. 2005).

In this study, the vicinity of the worm was continuously perfused via a two-channel gravity-fed system. The worm was stimulated by switching between the channels containing normal saline and repellent saline. Normal saline comprised (in mM): NaCl (50), $CaCl_2$ (0.1), sorbitol (100). To form the repellent saline, 10 mM $CuCl_2$ was added

to normal saline. Each animal was stimulated and recorded once, then discarded. In control experiments (Fig. 3A), both perfusion channels carried normal saline.

Approximately half the animals prepared in this way exhibited vigorous swimming behavior that had distinct forward and reverse states characterized, respectively, by a head-to-tail or tail-to-head progression of the body wave, as described previously (Faumont et al. 2005). The other animals appeared to move in an uncoordinated fashion, or not at all, so we excluded them. The proportion of vigorously swimming animals declined to zero in about 40 minutes. We attributed poor swimming behavior to the presence of glue on the animal because unglued individuals nearby in the recording chamber continued to swim normally; the AQ1444 strain appeared to be more sensitive to the glue than wild type worms for unknown reasons. This sensitivity is unlikely to result from expression of the cameleon protein because other cameleon-expressing strains do not display it (Faumont and Lockery, unpublished data).

Calcium imaging. Images were acquired using the MetaVue (version 6.2r2, Molecular Devices, Sunnyvale, CA). Frames were taken at a 1.25-33.0 Hz (corresponding to exposure times of 30-800 ms) with 8x8 spatial binning. This range of exposure times reflects the variability in the expression level of cameleon. Images stacks were processed using Jmalyze (written and kindly provided by Rex Kerr, Salk Institute, San Diego, CA), as described previously (Kerr et al. 2000; Suzuki et al. 2003). The YFP/CFP emission ratio was computed as (YFP intensity)/(CFP intensity) - 0.65, where the latter term corrects for CFP bleed-through into the YFP channel. The emission ratio

was compensated for photobleaching by fitting a single exponential function to the inactive portions of the emission ratio trace and dividing it by the fitted curve; thus, all ratio changes were expressed in terms of DR/R. A spurious ratio change was sometimes detected in ASH neurons immediately after exposure of the preparation to the cameleon excitation beam, as reported previously (Hilliard et al. 2005). This ratio change was accompanied by a modest increase in reverse swimming probability that decayed in ~5 sec. We therefore waited 15 sec after turning on the excitation beam before delivering the chemosensory stimulus. Spatial displacement of the neuron in the *x-y* plane was assessed by computing the radial distance between the present and initial positions of the cell body.

Behavioral analysis. Video recordings were digitized and replayed frame-by-frame to note the times at which transitions between forward and reverse swimming occurred (Faumont et al. 2005). The time of transition from forward to reverse swimming was defined as the frame in which there appeared in the tail a sharp inflection that grew into a coordinated, tail-to-head body wave (see supplemental movie). The time of transition from reverse to forward swimming was defined as the frame in which the flexed posture characteristic of reverse swimming began to unfold into a head-to-tail body wave. The probability of reverse swimming was computed in consecutive 5 sec bins as T_r / T, where T_r is total time in the reverse state, and T is bin length. Behavior scoring was not blind to the stimulus.

Statistics. In the lower panel of Fig. 3A1, differences between pairs of binwise means (stimulated vs. unstimulated; $t \geq 0$ sec) were assessed using multiple *t*-tests ($m = 6$). In accordance with the Bonferroni procedure (Winer et al. 1991) for a joint significance level of $P = 0.05$, the significance level required on individual tests was lowered from 0.05 to $1 - (1 - 0.05)^{1/m} = 0.0085$. The significance in the linear regressions of Figs. 3A2-3B2 was assessed according to the statistic $r\sqrt{(N-2)/(1-r^2)}$, which is distributed like Student's *t*-distribution with $N - 2$ degrees of freedom (Press et al. 1988).

Results

We first asked whether calcium signals could be detected reliably in semi-restrained worms. This question was significant because even when the cuticle of the worm's head is glued to the substrate, cells within the head often move as rest of the body flexes or extends, and cell movements are larger in the semi-restrained preparation used here than in the fully-restrained preparations typically used in *C. elegans* calcium imaging experiments.

We addressed the question of reliability by attempting to detect calcium signals in the ASH neurons, a left-right pair of sensory neurons that is sensitive to noxious chemical inputs and mechanosensory stimulation (Hart et al. 1995; Maricq et al. 1995; Sambongi et al. 1999). We selected ASH neurons for study because calcium signals have previously been obtained from them in fully-restrained worms (Hilliard et al. 2005), and because stimuli that activate ASH neurons also induce an avoidance response that is easy to observe and quantify in semi-restrained worms (Faumont et al. 2005). In response to the chemical repellant $CuCl_2$, each of the 27 ASH cells we imaged showed a clear ratio change that was characterized by a sharp rise and a prolonged decay, as exemplified by the recording shown in Fig. 2. The time course and amplitude of the ratio change were consistent with previously observed calcium transients in ASH neurons in fully restrained preparations (Hilliard et al. 2005).

It is well known, however, that calcium imaging is susceptible to movement artifacts. This is true even in the case of a ratiometric probe such as cameleon, where imperfections in background correction and chromatic aberration lead to spurious ratio changes, particularly for cell movements along the *z*-axis (Kerr 2002). To explore the question of whether the ratio changes we measured resulted from a change in calcium concentration or cell movement, we employed the usual procedure of inspecting the YFP and CFP intensity traces that underlie the ratio trace. Theoretically, changes in calcium concentration usually cause reciprocal changes in YFP and CFP intensity, whereas cell movements usually cause changes in the same direction (Kerr 2002). In about half of the ASH cells we recorded (13/27, 48%), reciprocal changes in YFP and CFP intensity were coincident with the ratio change (Fig. 2); these ratio changes were therefore likely to be the result of changes in calcium concentration. In the other cells, similar ratio changes were observed in the absence of reciprocal changes in YFP and CFP intensity. We believe that reciprocal changes in these cells were obscured by movement artifacts. In support of this view, a scatter plot of the data from all 27 ASH neurons (not shown) revealed that cells in which there was more movement in the *x*-*y* plane had higher joint variances in CFP and YFP intensities and were less likely to exhibit reciprocal changes. Nevertheless, the time course and amplitude of ratio changes in the non-reciprocal cases closely resembled the time course and amplitude in the reciprocal cases in this study, and in a previous one in which ASH neurons were imaged in fully-restrained worms (Hilliard et al. 2005). This resemblance suggests that the non-reciprocal ratio changes we saw were caused mainly by changes in calcium concentration, not movement artifacts, and we therefore included these data in our

analysis. We conclude that calcium transients can be detected reliably in semi-restrained worms.

We next asked whether behavioral responses persist in worms whose sensory neurons express cameleon, in the same set of 27 worms. This question was significant because cameleon, which contains the calcium binding protein calmodulin, could alter calcium concentration and its dynamics in the ASH neurons, which are responsible for triggering avoidance responses to $CuCl_2$. Most worms (18/27, 67%) appeared to respond to the repellent by making an avoidance response, defined as a transition from forward to reverse swimming, with a latency of less than 10 sec; one such response is illustrated in Fig. 2 and the supplemental movie. Of the other nine worms, six were engaged in a spontaneous bout of reverse swimming at the time the stimulus was delivered (so it was not possible to determine whether or not they responded to the stimulus), whereas three did not reverse. In addition, at the population level, we observed a significant increase in reverse swimming probability, relative to unstimulated control animals, in the 5 sec following stimulus onset (Fig. 3A; $t_{(33)} = 2.815$, $P = 0.008$). We conclude that avoidance responses persist in worms that express the cameleon protein in the sensory neuron responsible for this behavior.

To assess the relative utility of simultaneous versus non-simultaneous recordings, we analyzed the probability and ratio data in two different ways: first, using average probabilities and average ratios taken across animals (Fig. 3A) and, second, using probabilities and ratios taken from individual animals (Fig. 3B). The first method is

statistically equivalent to seeking correlations in calcium and behavioral data recorded non-simultaneously, i.e. from separate groups of animals, and serves as a point of comparison for the second method, which takes advantage of the dual-objective approach.

Using the first method, we plotted the average time course of the YFP/CFP ratio and the average time course of reverse swimming probability on the same time axis (Fig. 3A1). As noted above, this plot showed that a statistically significant increase in reverse swimming probability (relative to unstimulated controls) occurred in the first time bin after the stimulus, coinciding with the peak of the ASH calcium transient. However, a regression of average probability against average ratio demonstrated the absence of an overall correlation between calcium activity and behavior (Fig. 3A2; $r = 0.011$, $P = 0.98$). The absence of a correlation is somewhat surprising in light of previous evidence linking ASH neurons tightly to avoidance responses (Hart et al. 1999; Hilliard et al. 2002; Kaplan and Horvitz 1993; Maricq et al. 1995; Sambongi et al. 1999; Troemel et al. 1995). However, avoidance-response probability is also influenced by other neurons in *C. elegans* (Hilliard et al. 2002; Miller et al. 2005; Sambongi et al. 1999; Zariwala et al. 2003; Zheng et al. 1999).

Using the second method, we computed regressions of probabilities against ratios obtained simultaneously from individual worms in each of the 5 sec time bins before and after the stimulus. We found a significant positive correlation between probability and ratio in the time bin immediately after stimulus onset (Fig. 3B1, $r = 0.54$, $P = 0.008$), but

no significant correlations in the other time bins (Fig. 3B2, binwise *P*'s ≥ 0.07). Thus larger ASH calcium transients were associated with higher reverse swimming probability at precisely the time when reverse swimming probability was significantly elevated relative to unstimulated controls, suggesting that ASH contributes to the transient increase in reverse swimming probability. The fact that the second method was successful in revealing a correlation where the first method was not indicates that simultaneous recordings, made possible by the dual-objective approach, can detect subtle effects that may not be apparent in non-simultaneous recordings.

Discussion

This study demonstrates the practicality of making simultaneous recordings of neuronal calcium transients and whole-animal behaviors using the dual-objective approach. This is the first time simultaneous recordings have been reported for animals and neurons on a spatial scale as small as that of *C. elegans*. An analogous technique has been used to record calcium transients and behavior in larval zebra fish (Higashijima et al. 2003; Ritter et al. 2001).

The dual-objective approach has two distinguishing features. The first feature is the simultaneous use of two objectives: a low power, wide field objective for imaging behavior, and a high power, narrow field objective for imaging calcium transients. The second feature is the use of different wavelengths of light to prevent interference between the calcium imaging and behavioral optics. Wavelength separation was achieved by illuminating the preparation with red light, which was invisible to the calcium imaging optics. Conversely, a long pass filter prevented the fluorescence excitation light from reaching the behavior camera.

The new approach has two main limitations. First, it is restricted to behaviors that survive semi-restraint. In *C. elegans*, these include swimming, foraging, pharyngeal pumping, and egg laying. Second, it is restricted to recording neurons within, or quite near to, the glued region of the animal. In worms glued by the head for example, tail

neurons and many of the body-muscle motor neurons are likely to move too much to be imaged reliably.

The main advantage of the dual-objective approach is that it links with each frame in the optical recording of neural activity an image of the animal's behavior at the time the frame was captured. This linkage was achieved by synchronizing the starting point of the calcium and behavioral data streams and knowing the frame rates of the two data streams. By enabling us to plot probabilities against ratios obtained simultaneously from individual worms, the dual-objective approach revealed a correlation between reverse swimming probability and calcium transients in ASH chemosensory neuron that might otherwise have remained obscure. It should now be possible to seek correlations between the activity of other identified neurons and behavior in *C. elegans*.

The dual-objective approach is likely to be useful in many other types of experiments as well. These include situations in which it would be desirable to record simultaneously at two different spatial resolutions from a single location is space, such as when investigating the relationship between the activity of a single neuron and the network in which it is embedded, for example. Such experiments also include situations in which it would be desirable to record simultaneously from two different locations in space, such as when studying neurons separated by great distances, or a neuron and the appendage it controls. Finally, the dual-objective approach could also be adapted to photostimulation experiments in which the high power objective is used to excite the

phototrigger and the low power objective is used to observe the resulting network activity or behavior (Boyden et al. 2005; Lima and Miesenbock 2005).

Acknowledgements

We thank Christian Froekjaer-Jensen, Rex Kerr, William Schafer, and Hiroshi Suzuki for assistance with calcium imaging and Robert Hodges (SD Instruments, Grants Pass, OR) for custom apparatus.

Grants

This work was supported by National Institute of Mental Health Grant MH051383.

References

Boyden ES, Zhang F, Bamberg E, Nagel G, and Deisseroth K. Millisecond-timescale, genetically targeted optical control of neural activity. *Nat Neurosci* 8: 1263-1268, 2005.

Christensen M, Estevez A, Yin X, Fox R, Morrison R, McDonnell M, Gleason C, Miller DM, 3rd, and Strange K. A primary culture system for functional analysis of *C. elegans* neurons and muscle cells. *Neuron* 33: 503-514, 2002.

Davis MW, Somerville D, Lee RY, Lockery S, Avery L, and Fambrough DM. Mutations in the *Caenorhabditis elegans* Na/K-ATPase alpha-subunit gene, eat-6, disrupt excitable cell function. *J Neurosci* 15: 8408-8418, 1995.

Faumont S, Miller AC, and Lockery SR. Chemosensory behavior of semi-restrained *Caenorhabditis elegans*. *J Neurobiol* 65: 171-178, 2005.

Fiala A, Spall T, Diegelmann S, Eisermann B, Sachse S, Devaud JM, Buchner E, and Galizia CG. Genetically expressed cameleon in *Drosophila melanogaster* is used to visualize olfactory information in projection neurons. *Curr Biol* 12: 1877-1884, 2002.

Goodman MB, Hall DH, Avery L, and Lockery SR. Active Currents Regulate Sensitivity and Dynamic Range in *C. elegans* Neurons. *Neuron* 20: 763-772, 1998.

Guerrero G, and Isacoff EY. Genetically encoded optical sensors of neuronal activity and cellular function. *Curr Opin Neurobiol* 11: 601-607, 2001.

Hart AC, Kass J, Shapiro JE, and Kaplan JM. Distinct signaling pathways mediate touch and osmosensory responses in a polymodal sensory neuron. *J Neurosci* 19: 1952-1958, 1999.

Hart AC, Sims S, and Kaplan JM. Synaptic code for sensory modalities revealed by *C. elegans* GLR-1 glutamate receptor. *Nature* 378: 82-85, 1995.

Hasan MT, Friedrich RW, Euler T, Larkum ME, Giese G, Both M, Duebel J, Waters J, Bujard H, Griesbeck O, Tsien RY, Nagai T, Miyawaki A, and Denk W. Functional fluorescent Ca2+ indicator proteins in transgenic mice under TET control. *PLoS Biol* 2: e163, 2004.

Higashijima S, Masino MA, Mandel G, and Fetcho JR. Imaging neuronal activity during zebrafish behavior with a genetically encoded calcium indicator. *J Neurophysiol* 90: 3986-3997, 2003.

Hilliard MA, Apicella AJ, Kerr R, Suzuki H, Bazzicalupo P, and Schafer WR. In vivo imaging of *C. elegans* ASH neurons: cellular response and adaptation to chemical repellents. *Embo J* 24: 63-72, 2005.

Hilliard MA, Bargmann CI, and Bazzicalupo P. *C. elegans* responds to chemical repellents by integrating sensory inputs from the head and the tail. *Curr Biol* 12: 730-734, 2002.

Kaplan JM, and Horvitz HR. A dual mechanosensory and chemosensory neuron in Caenorhabditis elegans. *Proc Natl Acad Sci U S A* 90: 2227-2231, 1993.

Kerr R. Imaging Excitable Cell Activity in *C. elegans*. In: *Department of Biology*. San Diego, CA: University of California, 2002.

Kerr R, Lev-Ram V, Baird G, Vincent P, Tsien RY, and Schafer WR. Optical imaging of calcium transients in neurons and pharyngeal muscle of *C. elegans*. *Neuron* 26: 583-594, 2000.

Lima SQ, and Miesenbock G. Remote control of behavior through genetically targeted photostimulation of neurons. *Cell* 121: 141-152, 2005.

Maricq AV, Peckol E, Driscoll M, and Bargmann CI. Mechanosensory signaling in *C. elegans* mediated by the GLR-1 glutamate receptor. *Nature* 378: 78-81, 1995.

Miesenbock G. Genetic methods for illuminating the function of neural circuits. *Curr Opin Neurobiol* 14: 395-402, 2004.

Miesenbock G, and Kevrekidis IG. Optical imaging and control of genetically designated neurons in functioning circuits. *Annu Rev Neurosci* 28: 533-563, 2005.

Miller AC, Thiele TR, Faumont S, Moravec ML, and Lockery SR. Step-response analysis of chemotaxis in *Caenorhabditis elegans*. *J Neurosci* 25: 3369-3378, 2005.

Miyawaki A. Fluorescence imaging of physiological activity in complex systems using GFP-based probes. *Curr Opin Neurobiol* 13: 591-596, 2003.

Miyawaki A, Griesbeck O, Heim R, and Tsien RY. Dynamic and quantitative Ca2+ measurements using improved cameleons. *Proc Natl Acad Sci U S A* 96: 2135-2140, 1999.

Miyawaki A, Llopis J, Heim R, McCaffery JM, Adams JA, Ikura M, and Tsien RY. Fluorescent indicators for Ca2+ based on green fluorescent proteins and calmodulin. *Nature* 388: 882-887, 1997.

Ng M, Roorda RD, Lima SQ, Zemelman BV, Morcillo P, and Miesenbock G. Transmission of olfactory information between three populations of neurons in the antennal lobe of the fly. *Neuron* 36: 463-474, 2002.

Press WH, Flannery BP, Teukolsky SA, and Vetterling WT. *Numerical Recipes in C*. Cambridge: Cambridge University Press, 1988.

Richmond JE, and Jorgensen EM. One GABA and two acetylcholine receptors function at the C. elegans neuromuscular junction. *Nat Neurosci* 2: 791-797, 1999.

Ritter DA, Bhatt DH, and Fetcho JR. *In vivo* imaging of zebrafish reveals differences in the spinal networks for escape and swimming movements. *J Neurosci* 21: 8956-8965, 2001.

Sambongi Y, Nagae T, Liu Y, Yoshimizu T, Takeda K, Wada Y, and Futai M. Sensing of cadmium and copper ions by externally exposed ADL, ASE, and ASH neurons elicits avoidance response in *Caenorhabditis elegans*. *Neuroreport* 10: 753-757, 1999.

Suzuki H, Kerr R, Bianchi L, Frokjaer-Jensen C, Slone D, Xue J, Gerstbrein B, Driscoll M, and Schafer WR. In vivo imaging of *C. elegans* mechanosensory neurons demonstrates a specific role for the MEC-4 channel in the process of gentle touch sensation. *Neuron* 39: 1005-1017, 2003.

Troemel ER, Chou JH, Dwyer ND, Colbert HA, and Bargmann CI. Divergent seven transmembrane receptors are candidate chemosensory receptors in *C. elegans*. *Cell* 83: 207-218, 1995.

Winer BJ, Brown DR, and Michels KM. *Statistical Principles in Experimental Design*. Boston: McGraw-Hill, 1991.

Zariwala Z, Miller A, Faumont S, and Lockery S. Step response analysis of thermotaxis in *C. elegans*. *J Neurosci* in press: 2003.

Zheng Y, Brockie PJ, Mellem JE, Madsen DM, and Maricq AV. Neuronal control of locomotion in *C. elegans* is modified by a dominant mutation in the GLR-1 ionotropic glutamate receptor. *Neuron* 24: 347-361, 1999.

Legends

Fig. 1. Schematic diagram of the dual-objective approach. An inverted compound microscope (not shown) with epifluorescence illumination and a high power objective for neuronal imaging was fitted with a hinged platform carrying a low power objective, filter, and camera for monitoring behavior. The preparation ("worm") was illuminated from the side by a red laser beam.

Fig. 2. Simultaneous recording of calcium transients and behavior using the dual-objective approach. The animal was exposed to a 0 to 10 mM step in the concentration of $CuCl_2$, an aversive compound that induces avoidance responses in the form of reverse swimming behavior. The YFP and CFP traces show, respectively, the fluorescence intensity of the yellow and cyan components of the cameleon probe. The DR/R trace shows the YFP/CFP intensity ratio, which indicates the relative calcium concentration in the cell body of the neuron; the ratio at each time point was normalized to the inactive region of the trace, as a correction for optical bleaching of the probe. The displacement trace shows the distance by which the center of the neuron moved during the experiment. Behavioral state is shown by the black and white bars at the bottom of the figure. The delay between stimulus onset and the calcium transient reflects the latency of solution exchange an sensory transduction in ASH neurons.

Fig. 3. Correlations between neuronal activity and behavior. A1. Average ratio and average reverse swimming probability as a function of time relative to the onset of the

aversive stimulus $CuCl_2$. Average ratio-changes were obtained by computing, for each animal, the time-averaged ratio change in successive 5 sec bins, and taking bin-wise averages across animals. Average probabilities were obtained by computing, for each animal, the fraction of time spent in the reverse swimming state in each bin, and taking bin-wise averages across animals. Filled and open symbols indicate behavior in the presence and absence of the stimulus, respectively. The uppermost trace represents the stimulus. Bars are SEM and the asterisk indicates significance at the $P < 0.05$ level in *t*-tests corrected for multiple comparisons. A2. Regression of average reverse swimming probability against average ratio. The line is the least squares linear fit to the data. B1. Regression of reverse swimming probabilities against ratios obtained simultaneously from individual worms in the 5 sec bin immediately following stimulus onset. The line is the least squares linear fit to the data. B2. Correlation coefficients as a function of time relative to the onset of the aversive stimulus. The asterisk indicates a significant correlation ($P < 0.01$). The uppermost trace represents the stimulus.

Supplementary Movie 1. Real-time movie of a glued worm swimming in the superfusion chamber. Traces show (top to bottom): [$CuCl_2$] (in mM), YFP and CFP intensities (in arbitrary units), and their ratio (expressed as $0R/R$). The moving cursors on the YFP, CFP, and DR/R traces indicate the value in trace for the corresponding movie frame. The behavioral state of the animal (*forward* swimming or *reversal*) is indicated at the side of the movie window. An increase in [$CuCl_2$] results in reciprocal changes in the YFP and CFP traces, leading to an increase in DR/R. This increase is associated with a behavioral switch from forward swimming to reverse swimming. The delay between

stimulus onset and the calcium transient reflects the latency of solution exchange an sensory transduction in ASH neurons. The movie animates the data as of Fig. 2 of the main text.

Figure 1

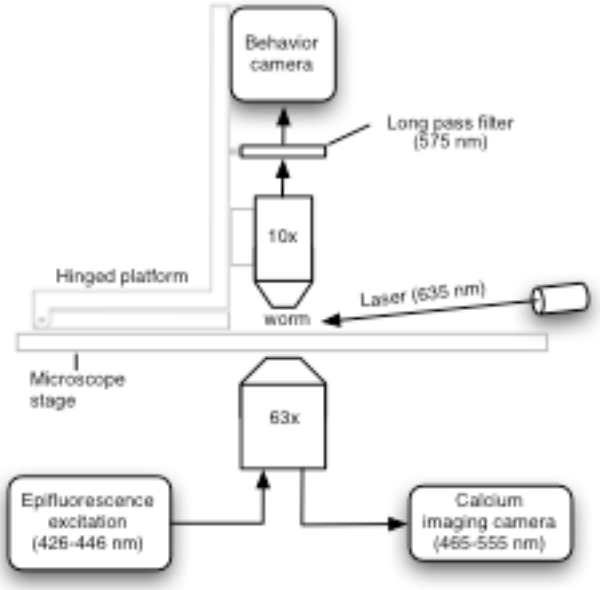
Behavior camera
Long pass filter (575 nm)
10x
Hinged platform
Laser (635 nm)
worm
Microscope stage
63x
Epifluorescence excitation (426-446 nm)
Calcium imaging camera (465-555 nm)

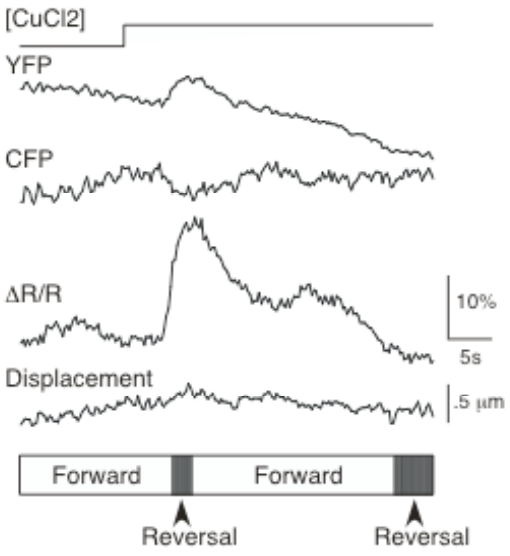
[CuCl2]
YFP
CFP
ΔR/R
10%
5s
Displacement
.5 μm
Forward
Forward
Reversal
Reversal

Figure 2

Figure 3

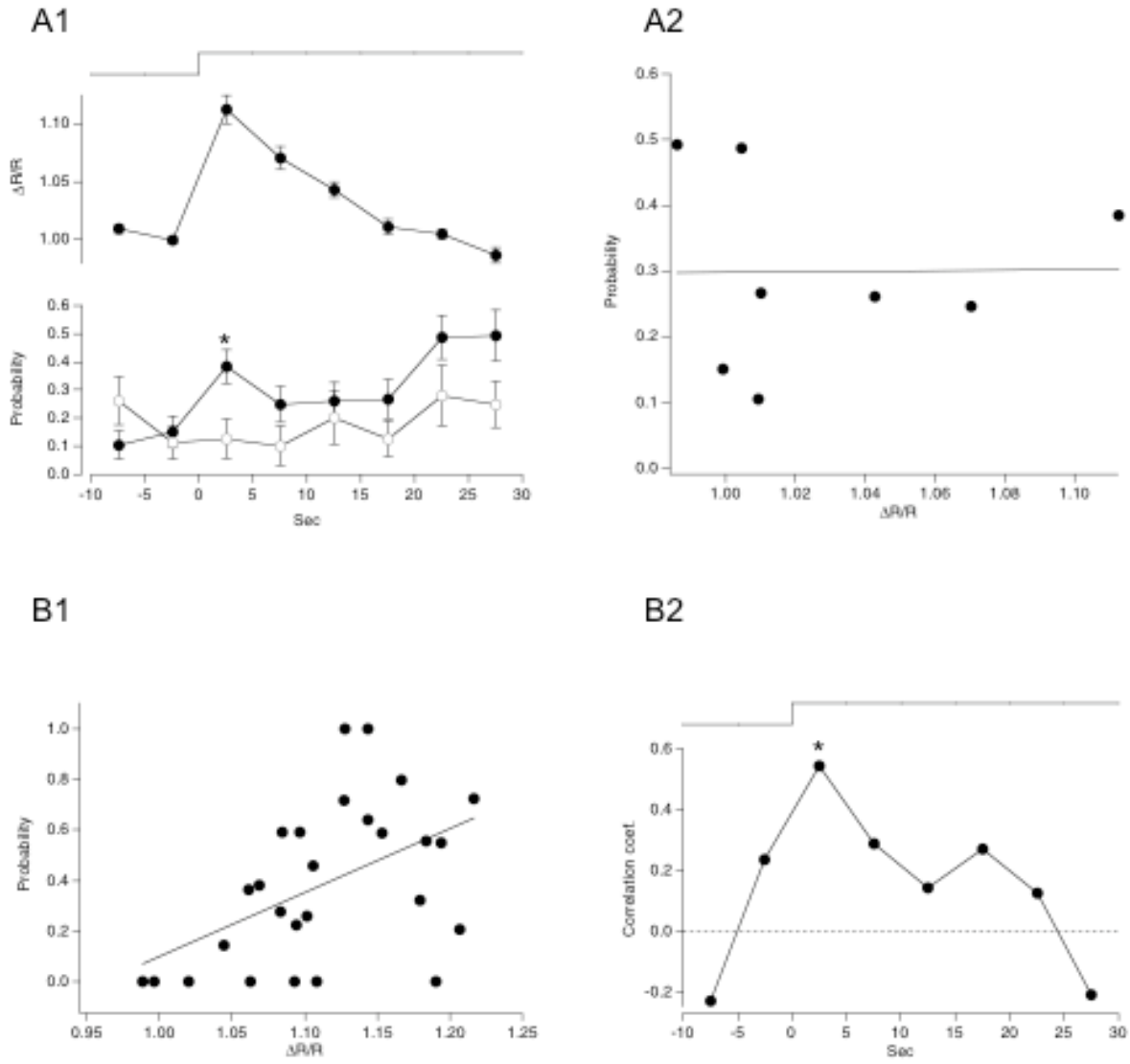
A1
ΔR/R
Probability
Sec
A2
Probability
ΔR/R
B1
Probability
ΔR/R
B2
Correlation coef.
Sec